Structural Analyses and Triacylglycerol Polymorphs with FT-IR Techniques. 2. β'_1-Form of 1,2-Dipalmitoyl-3-myristoyl-*sn*-glycerol

Junko Yano, Fumitoshi Kaneko,* and Masamichi Kobayashi

Department of Macromolecular Science, Graduate School of Science, Osaka University, Toyonaka, 560 Japan

Dharma R. Kodali

Central Research, Cargill Inc., Minneapolis, Minnesota 5544-5699

Donald M. Small

Department of Biophysics, Housman Medical Research Center, Boston University School of Medicine, 80 East Concord Street, Boston, Massachusetts 02118

Kiyotaka Sato

Faculty of Applied Biological Science, Hiroshima University, Higashi-Hiroshima 739, Japan

Received: April 15, 1997; In Final Form: July 21, 1997[⊗]

On the basis of the assignments of the methylene wagging bands described in the preceding paper (Part 1), FT-IR studies have been applied to the β'_1-form of 1,2-dipalmitoyl-3-myristoyl-*sn*-glycrerol (PPM). PPM has the most stable form of β'-type, in contrast to ordinary triacylglycerols, which have the most stable form of β-type. The degrees of inclination of the acyl chains with respect to the lamellar interface were determined by two FT-IR techniques of attenuated total reflection and oblique transmission. The acyl chains were packed in orthorhombic perpendicular ($O_\perp$) subcell as revealed in the absorption spectra of polymethylene scissoring and rocking modes. As for the acyl chain conformation, it was found that a palmitoyl chain and a myristoyl chain extend to form an all-*trans* conformation, while the second palmitoyl chain takes a bent conformation in the neighborhood of the ester bond. The acyl chain axis tilts against both the a_s- and the b_s-axis of the $O_\perp$ subcell, yet the degree of inclination against the b_s-axis is slightly larger than that against the a_s-axis. The a_s-axis is inclined unidirectionally, while the b_s-axis is alternately inclined along the successive layer.

Introduction

Triacylglycerols (TAGs) are major fats present in biotissues, food materials, and pharmaceuticals. The importance of structural determination of TAG crystals at a molecular level has been described in a preceding paper (Part 1)[1] and in the literature.[2−5]

Major interests of the molecular structural analyses of TAGs may be categorized into two groups: (a) polymorphism revealing three typical forms of α, β', and β, and (b) symmetry in distribution of the fatty acyl chains bound to three glycerol carbons in the case that one molecule contains different types of acyl chains.

As for the first category of interests, precise crystal structures with an X-ray diffraction method have been solved only for the most stable β-form.[6,7] Although the β'-forms are more important than the β-forms because of their functional physical properties such as crystal morphology, crystallization rate, crystal network formation, etc.,[4,5] no convincing structural data are available.[8] The main problems inherent to the β' structures are the conformation of acyl chains and glycerol groups, subcell structure, chain inclination, and multiplicity in the occurrence of the β'-forms. NMR spectroscopy has shown that the molecular motions of the acyl chains of β' are more restricted than those of α, but more enhanced than those of β.[9,10] As for the glycerol conformation, it concerns the arrangement of the three acyl chains connected to the three glycerol carbons in the chairlike molecular structure, with regard to two possibilities: *sn*-1,3 and *sn*-1,2 configurations. The former means that the acyl chains at the glycerol carbon positions of *sn*-1 and *sn*-3 are adjacent, while the *sn*-2 chain is protruding to the opposite side. By contrast, the acyl chains at the *sn*-1 and *sn*-2 are adjacent in the latter arrangement. The β-forms of monoacid TAGs are arranged in this type as proved by the X-ray structure analysis.[6,7] As for the subcell structure, all of the β'-forms were assumed to be the orthorhombic perpendicular ($O_\perp$) subcell. The occurrence of the plural β'-forms has been reported in the monoacid and mixed-acid TAGs.[4,11,12]

The symmetry in the acyl chain distribution is a vital subject for most of the TAGs present in biological and industrial systems, since these TAGs contain different types of fatty acids consisting of short and long chains, saturated and unsaturated acids, etc. In particular, the natural fats usually contain a large amount of asymmetric TAGs, where the glycerol carbon positions of *sn*-1,2, and 3 connected to fatty acids of different species are not symmetric. An interesting point is that the symmetry in the acyl chain distribution is often related to the polymorphic behavior of TAGs. For example, the β'-forms are most stable in certain types of asymmetric mixed-acid TAGs. In this specific case, the difficulty of growing single crystals of β' is eliminated, and the structural studies are enabled. The typical materials exhibiting these properties are a series of TAGs called PP*n*, in which the *sn*-1,2 positions contain palmitoyl chains and the numbers (*n*) of carbon atoms of the fatty acids at the *sn*-3 position vary from 2 to 14.[11−14]

* Corresponding author. Fax: +81-6-850-5453.

[⊗] Abstract published in *Advance ACS Abstracts,* September 15, 1997.

S1089-5647(97)01305-9 CCC: $14.00

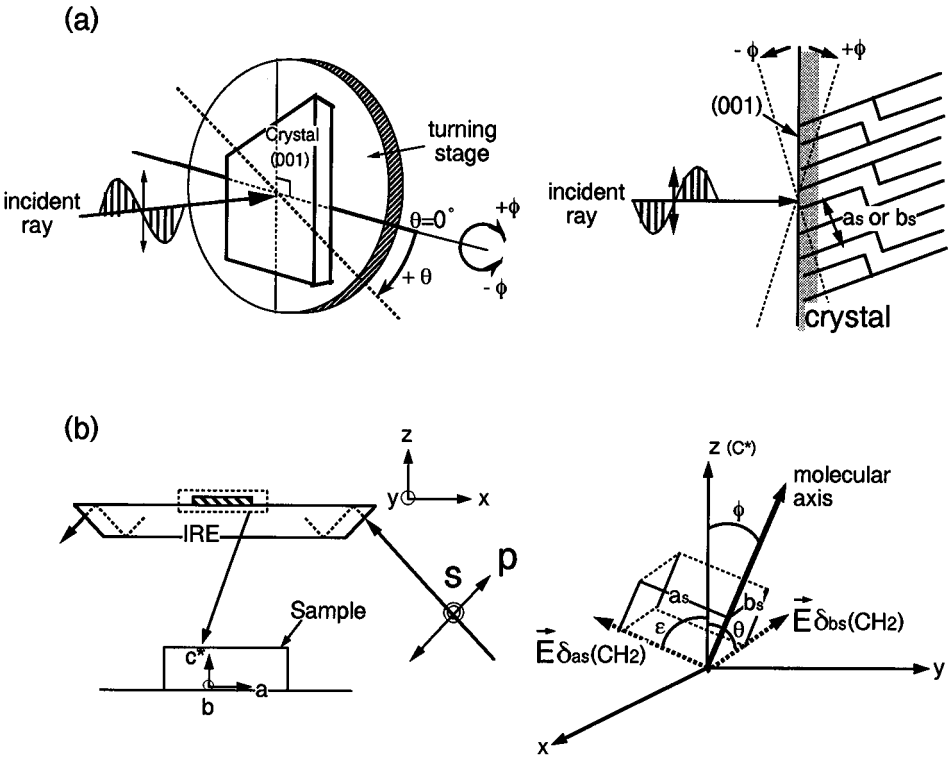

Figure 1. Schematic representation of (a) the oblique transmission and (b) ATR.

The β'-form becomes stable in PP6, PP8, and PP14. For example, PP14 (PPM; 1,2-dipalmitoyl-3-myristoyl-*sn*-glycerol) has three forms called α, β'_2, and β'_1: α with $T_m = 39.5$ °C, β'_2 with $T_m = 56.0$ °C, and β'_1 with $T_m = 58.6$ °C (T_m, melting point).[12] The subcell structure of the two β'-forms is $O_\perp$, and the lamellar thickness corresponds to the double-chain length,[12] but the detailed structure on a molecular level remains unclear. Recently, tiny single crystals of the most stable β'_1-form of PPM were grown from solution by the present authors. The crystals exhibit slender rhombic morphology having the interplanar angles of 123° and 57°, which are nearly the same as those of β-forms observed in the monoacid TAGs. Although the size and crystallinity of the crystals available are not enough for the X-ray structural analysis, vibrational spectroscopy could be applied.

The main purpose of the present work was aimed at analyzing the molecular structures using infrared (IR) absorption spectroscopy with the use of methylene progression bands due to ν_3 (wagging modes), ν_7 (twisting−rocking modes), and ν_8 (rocking modes) branches, which were reported in Part 1. It was found that a series of IR progression bands of the two straight *sn*-1 and *sn*-2 chains of monoacid TAGs β-forms were different in frequency from those of the bent *sn*-3 chain having a *gauche* conformation in the neighborhood of the ester bond. It follows that the frequency difference in the progression bands between the straight and bent chains observed in the β-forms (Part 1) can be applied to complicated TAG polymorphs, especially for the asymmetric mixed-acid TAGs. Among the several series of progression bands in TAGs, the ν_3 bands were suitable to assess the acyl chain conformation because of the following two reasons: (1) both of the ν_3 bands of the straight and bent chains were isolated with detectable intensity, and (2) the transition dipole moments of the ν_3 bands have a large component parallel to the chain axis, suggesting that the intermolecular interactions in the lateral directions had no significant influence on the ν_3 bands.

The objective of the present study was to clarify the molecular structures of the β'_1-form of PPM using various FT-IR techniques. Primary concerns are the subcell structure, the acyl chain configuration, and the mode of chain inclination.

Experiments

Samples. PPM (1,2-dipalmitoyl-3-myristoyl-*sn*-glycerol) was synthesized according to the method described previously.[13] Single-crystal specimens of β'_1 were crystallized from acetonitrile solutions by slow cooling. The polymorphic form was confirmed by the crystal morphology, X-ray diffraction (XRD) pattern, and melting point measured by a Rigaku DSC-8230.

XRD Measurements. The X-ray diffraction method was employed to obtain the lamellar thickness. The spectra were measured for two types of samples, well-oriented specimen (single-crystal mat grown from an acetonitrile solution) and powder crystals in order to distinguish the (00*l*) reflections. The former was measured by a Rigaku Rotaflex XRD (RU 200, Cu-Kα, 50 kV, 150 mA). The latter was packed in a thin-walled quartz capillary tube (diameter, 1 mm) and measured by a Rigaku Rotaflex XRD (RINT 2500, Cu-Kα, 50 kV, 300 mA).

IR Measurements. Transmission IR spectra were taken with a Degilab FTS60A spectrometer. An Oxford flow type cryostat CF1104 and an Oxford temperature controller ITC-4 were used for low-temperature measurements. Reflection-absorption spectroscopy (RAS) and attenuated total reflection (ATR) measurements were carried out with a JASCO FT-IR 8300 spectrometer with its accessories. Polarized IR spectra were taken with a MCT detector and a wire-grid polarizer (JASCO PR500).

A specimen for RAS was built up as a thin film by developing a chloroform solution on a flat aluminum plate.[1] By controlling the temperature of the metal substrate during the evaporation of chloroform, a thin film of β'_1 was formed reproducibly.

For the oblique transmission measurement,[15,16] the arrangement of a single-crystal specimen was changed with two axes, ϕ and θ, depicted in Figure 1a. At first, the θ axis was adjusted with the normal incident arrangement, $\phi = 0°$, to set the crystal at a suitable position for the oblique measurement, and then

the specimen was tilted with angle of ϕ within the plane including a subcell axis (a_s or b_s) and the polarized incident radiation.

Polarized ATR Measurements. To evaluate the inclination of acyl chain quantitatively, p- and s-polarized ATR spectra were measured.[17−18] The analysis was done according to the theory of Flournoy.[19,20] Under the assumption that the three axes of the specimen (*a*, *b*, and *c**) are arranged on IRE as shown in Figure 1b, the extinction coefficients (k_x, k_y, and k_z) of the films along the three axes (*x*, *y*, and *z*) are calculated from polarized ATR spectra. The extinction coefficient (k) is related to the Lambert's absorption coefficient (α) as

$$\alpha = 4\pi k/\lambda \tag{1}$$

where λ is the wavelength of radiation. The relationship between the absorbance (A), the reflectivity (R), and the extinction coefficient is given by the following equation for perpendicular (p) and parallel (s) polarization:

$$A_s = -\log R_s = \log e \cdot ak_y \tag{2}$$

and

$$A_p = -\log R_p = \log e \cdot (bk_x + ck_z) \tag{3}$$

In the above equations, the values of *a*, *b*, and *c* are given by

$$a = \frac{4n_2^2}{n_1^2 \tan\theta\left(1 - \frac{n_2^2}{n_1^2 \sin^2\theta}\right)^{1/2}\left(1 - \frac{n_2^2}{n_1^2}\right)} \tag{4}$$

$$b = \frac{4n_2^2\left(1 - \frac{n_2^2}{n_1^2 \sin^2\theta}\right)}{n_1^2 \tan\theta\left(1 - \frac{n_2^2}{n_1^2 \sin^2\theta}\right)^{1/2}\left(1 - \frac{n_2^2}{n_1^2 \sin^2\theta} + \frac{n_2^4}{n_1^4}\cot^2\theta\right)} \tag{5}$$

and

$$c = \frac{4n_2^2}{n_1^2 \tan\theta\left(1 - \frac{n_2^2}{n_1^2 \sin^2\theta}\right)^{1/2}\left(1 - \frac{n_2^2}{n_1^2 \sin^2\theta}\frac{n_2^4}{n_1^4}\cot^2\theta\right)} \tag{6}$$

where n_1 and n_2 are the refractive indices of the IRE and the film, respectively, and θ is the angle of incidence. In the present study, the film was built up on the sampling plane of the IRE (Ge) by developing the chloroform solution (Figure 1b, left). In this case, very fine uniaxially oriented crystals were generated. The lamellar stacking direction (*c**) is parallel to the *z*-axis, and the *a*- and *b*-axes of the crystals are distributed uniformly in the *xy*-plane. Therefore, the *x*-component (k_x) equals the *y*-component (k_y). Under the assumption that the refractive indices of Ge (n_1) and β'_1 (n_2) and incident angle θ were 4.0 and 1.5,[21] and 45°, respectively, we obtained the values of k_x (=k_y) and k_z from the intensity of A_s and A_p of $\delta(CH_2)$ bands. The angle ϵ between the *z*-axis and the transition moment of $\delta_{a_s}(CH_2)[\vec{E}\delta_{a_s}(CH_2)]$ and the angle θ between the *z*-axis and the transition moment of $\delta_{b_s}(CH_2)$ $[\vec{E}\delta_{b_s}(CH_2)]$ (Figure 1b, right), are given by

$$(k_z/k_x)_{a_s} = 2\cot^2\epsilon \tag{7}$$

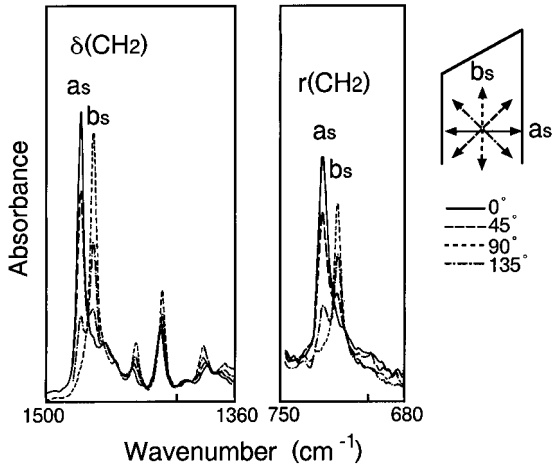

Figure 2. Polarized IR spectra of the β'_1-form in CH_2 scissoring and CH_2 rocking regions.

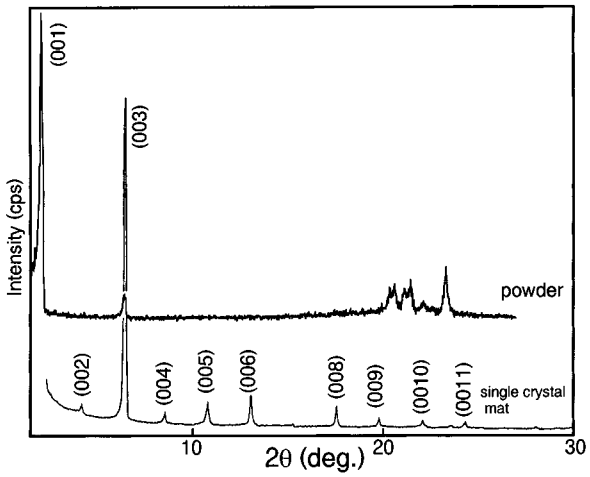

Figure 3. X-ray diffraction patterns of the β'_1-form.

and

$$(k_z/k_x)_{b_s} = 2\cot^2\theta \tag{8}$$

Then, the angle ϕ between the *z*-axis and molecular chain axis is calculated from the equation

$$\cos^2\epsilon + \cos^2\theta + \cos^2\phi = 1 \tag{9}$$

Results

Crystal Morphology and Subcell Orientation. The shape of the β'_1 crystal is a parallelogram whose acute angle is 57°. The CH_2 scissoring $\delta(CH_2)$ and CH_2 rocking $r(CH_2)$ bands of the $O_\perp$ subcell show clear dichroism for the single crystals of β'_1 (Figure 2).[22] The relation between the crystal morphology and the polarization of the incident radiation is depicted at the top right-hand corner of Figure 2. The a_s-components, 730 cm^{-1} ($r_{a_s}(CH_2)$) and 1473 cm^{-1} ($\delta_{as}(CH_2)$) bands, appear most intense at $\theta = 0°$ and vanish at $\theta = 90°$, while the intensity of the b_s-components, 720 cm^{-1} ($r_{b_s}(CH_2)$) and 1463 cm^{-1} ($\delta_{bs}(CH_2)$) bands, is maximum at $\theta = 90°$ and minimum at $\theta = 0°$ (the setting of the $O_\perp$ subcell follows orthorhombic polyethylene subcell determined by Bunn[23]). Therefore, the projections of the a_s- and b_s-axes of the $O_\perp$ subcell are almost perpendicular and parallel to the long axis of the single crystal.

Chain Length Structure. Figure 3 shows the XRD patterns of the PPM β'_1-form of the two samples: single crystal mat and powder specimens. The lamellar thickness (*d*(001) spacing)

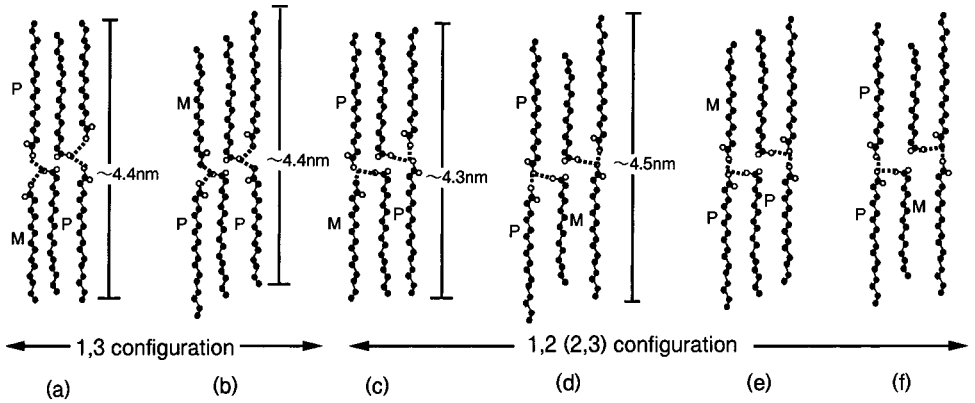

Figure 4. Schematic representation of the molecular structure of the β'-form of PPM. On the basis of the estimation that the lengths of the glycerol moieties in the *sn*-1,3 and the *sn*-1,2 configurations are about 0.5 and 0.4 nm, respectively, the molecular lengths of these forms can be roughly estimated as ~4.4 nm for types a and b, ~4.3 nm for types c and e, and ~4.5 nm for types d and f.

estimated from the $d(00l)$ reflections is 4.02 nm, corresponding to the double-chain length.[12]

On the basis of the double-chain-length structure, Figure 4 depicts possible six types of glycerol configurations; types a and b are classified as the *sn*-1,3 configuration and others as the *sn*-1,2 (or *sn*-2,3) configuration. In types a, b, c, and e, palmitoyl and myristoyl chains have the all-*trans* conformation, but the second palmitoyl chain has the bent conformation. On the other hand, two palmitoyl chains are fully extended, but a myristoyl chain has the bent conformation in types d and f. A total length composed of two palmitoyl chains including a glycerol moiety (types d and f) is assumed to be ~4.5 nm, while the values for types a, b, c, and e are 4.3−4.4 nm when the acyl chains of constituent fatty acids take the all-*trans* conformation. These values are longer than that of the observed lamellar thickness by approximately 0.25−0.4 nm, indicating that the acyl chains of β'_1 are inclined with respect to the (001) plane.

Acyl Chain Configuration. Using the ν_3 progression bands appearing in the 1360−1150 cm^{-1} region, we evaluated the postulated acyl chain configurations illustrated in Figure 4. Type a, b, c, or e must provide the progression bands arising from straight palmitoyl and myristoyl chains together with one bent palmitoyl chain. On the other hand, the progression bands of types d or f may consist of the bands arising from two straight palmitoyl chains and one bent myristoyl chain. The ν_3 bands of the straight chains mainly appear in RAS due to the transition dipole moment parallel to the chain axis. On the other hand, those of the bent chains, which involve a perpendicular component to the chain axis due to the bent conformation, strongly appear in transmission spectra.[1] Taking into account the difference in the polarization direction of the ν_3 bands from the two types of chains, we assigned the ν_3 bands of β'_1 to the results of trimyristin (MMM) and tripalmitin (PPP).[1]

Figure 5A shows the normal incident transmission spectra taken at 87 K and RAS taken at 297 K. In the specimen for RAS, the lamellar interface is parallel, and thereby the chain axes are almost normal to the metal surface. Accordingly, the bands whose transition moments are parallel to the chain axis are emphasized with a strong electron field normal to the metal surface. The comparison in the range of 1360−1150 cm^{-1} indicated that the marked bands with * in the transmission spectra correspond to the bands observed in RAS, meaning that the transition dipole moments of these bands mainly involve the components parallel to the chain axis. Therefore, these bands were assigned to the ν_3 progression bands due to the palmitoyl and/or myristoyl chain. In order to distinguish the contributions from these two chains, the frequencies of RAS bands were compared with those of the β-forms of PPP and MMM (Figure 5B). The bands marked with closed circles of PPP and MMM arise from the ν_3 bands of the straight palmitoyl and myristoyl chains.[1] It is noted that the bands in β'_1 totally correspond to the ν_3 bands of the straight chains of PPP and MMM. As for the composition of the bent chain, Figure 5C shows the comparison of the transmission spectra of the β'_1-form with those of the β-forms of PPP and MMM. The bands marked with open circles reveal the ν_3 bands of the bent palmitoyl and myristoyl chains. Meanwhile, the bent ν_3 bands marked with open circles in PPP correspond to those observed in the $\theta = 0°$ polarized spectrum of PPM β'_1 as connected by the dotted lines. No band series of the bent conformation of myristoyl moieties whose band positions were indicated by the broken lines was observed in the β'_1-form. For example, the strongest ν_3 band of the bent myristoyl chain at 1276 cm^{-1} was not observed in the spectra of PPM β'_1. The band frequencies in this region are listed in Table 1 together with the result of the ν_3 band assignments.

From the above discussion, we conclude that a palmitoyl chain takes the bent conformation, and the other palmitoyl and the myristoyl chains assume the all-*trans* conformation. This conclusion agrees with the acyl chain configurations of types a, b, c, and e in Figure 4.

Molecular Inclination Direction. The information on the inclination direction of the acyl chain was obtained by the oblique transmission, RAS, and ATR methods. Since the subcell orientation is directly related to the inclination direction of acyl chains, $\delta(CH_2)$ and $r(CH_2)$ bands having the transition dipole moments perpendicular to the molecular chain axis were employed as the reference bands of chain inclination direction.

Figure 6 shows the oblique transmission spectra of the β'_1-form. In Figure 6a, the electric vector $\vec{E}$ of the incident radiation and the a_s-axis of the $O_\perp$ subcell are in the same plane, and the angle that the a_s-axis and the electric vector make is varied by tilting the specimen (a_s-inclination). In contrast, the spectra in Figure 6b were taken with the inclination in the plane involving the b_s-axis and the electric vector (b_s-inclination).

With alternation of ϕ values in the a_s-inclination, the intensity of $\delta_{a_s}(CH_2)$ and $r_{a_s}(CH_2)$ bands significantly changed, being strongest at $\phi = 0°$. It is notable that an increase in the changes in band intensity due to the inclination angles of $+30°$ and $-30°$ are not symmetric; the former is larger than the latter. This implies that the a_s-axis is slightly inclined with respect to the (001) plane (Figure 6c). On the contrary, no remarkable changes were observed in the absorption intensity of the b_s-components, $\delta_{b_s}(CH_2)$ and $r_{b_s}(CH_2)$, in the b_s-inclination. This behavior suggested the two possibilities: the b_s-axis is parallel to the

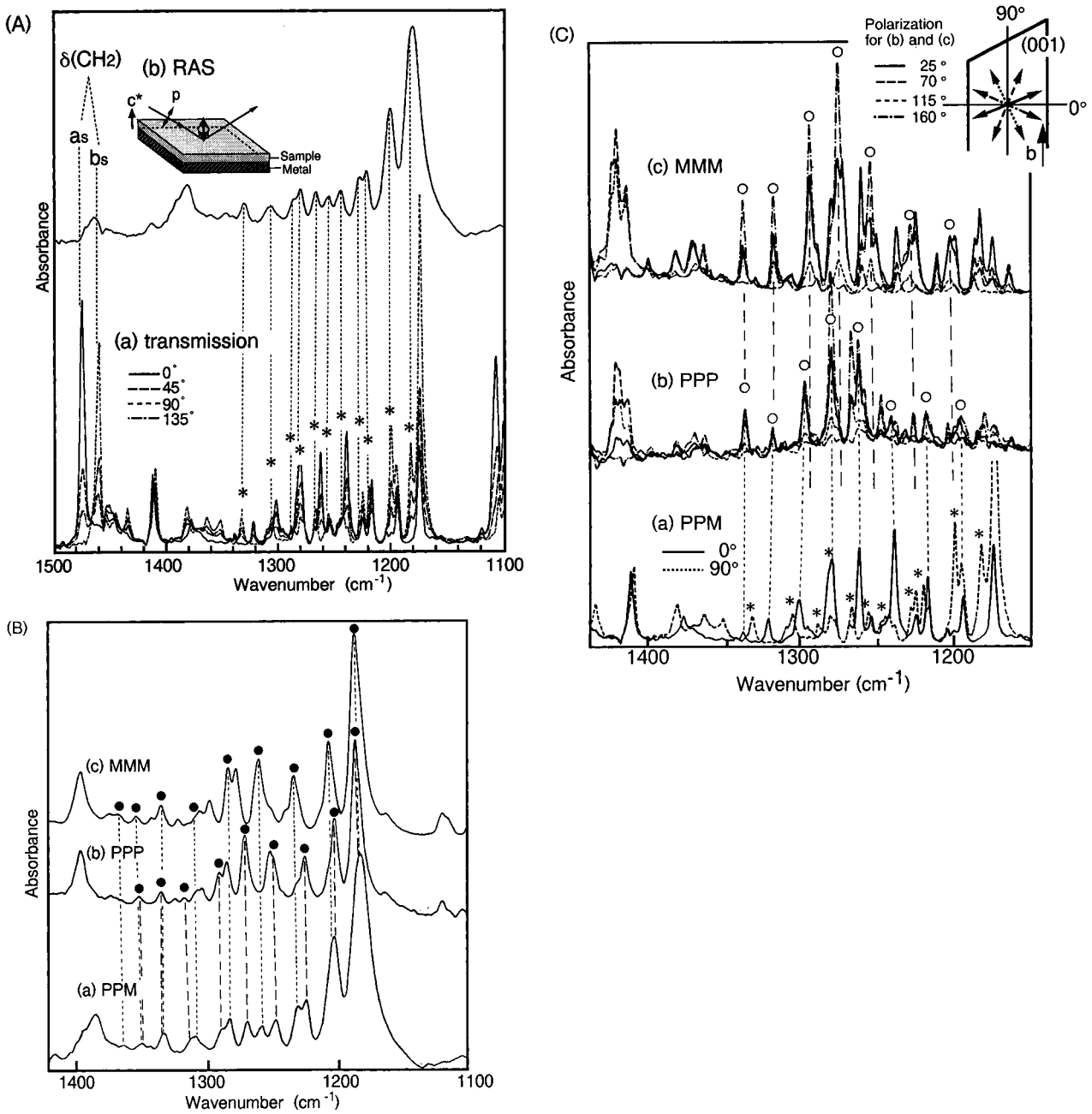

Figure 5. Assignments of the ν_3 progression bands of PPM β'_1: (A) IR spectra of β'_1 measured by (a) the normal incident transmission method (87 K) and (b) RAS (297 K), (B) RAS of PPM β'_1, PPP β, and MMM β, and (C) polarized normal incident transmission spectra of β'_1 of PPM (a) and β of PPP (b) and MMM (c) measured at 87 K. In (A) and (C), the bands marked with * correspond to the bands having detectable intensity in RAS. In (B) and (C), the assignments of the ν_3 progression bands of MMM and PPP are indicated: closed circles, the ν_3 bands of the straight chains; open circles, the ν_3 bands of the bent chains.

(001) plane, or it inclines alternately against the (001) plane. The results obtained from RAS and ATR spectra support the second possibility.

Since the component perpendicular to the (001) plane of a transition moment is only measurable with RAS, the perpendicular arrangement of the acyl chain exhibits no $\delta(CH_2)$ and $r(CH_2)$ bands. However, the b_s and a_s-components of $\delta(CH_2)$ appeared at 1473 and 1465 cm^{-1} and the b_s-component of $r(CH_2)$ at 720 cm^{-1} (Figure 7). The b_s-component was stronger in intensity than the a_s-component. This indicates that both the a_s- and b_s-axes are inclined, yet the b_s-axis is more inclined than the a_s-axis. Therefore, we infer that the unchanged intensities of the b_s-components shown in Figure 6b are ascribed to such an inclination behavior that the b_s-axis inclines toward the opposite directions alternately along the successive layer (Figure 6d).[15] In this type of stacking mode, the b_s-components of $\delta(CH_2)$ and $r(CH_2)$ due to the A-leaflet become weak at $\phi = +30°$, while they increase at $\phi = -30°$. On the other hand, the b_s-components due to the B-leaflet increase in intensity at $\phi = +30°$, while they decrease at $\phi = -30°$. Therefore, it results in the unchanged intensity, by canceling out, of the δ_{b_s}-(CH_2) and $r_{b_s}(CH_2)$ bands with the alternation of ϕ values.

The polarized ATR spectra also supported the above conclusion (Figure 8). The values of extinction coefficient k_x $(=k_y)$ and k_z for the a_s and b_s-components of the $\delta(CH_2)$ mode are summarized in Table 2. The direction of the transition dipole moment of each mode with respect to the *z*-axis was calculated from eqs 2−8; $\epsilon = 82.3°$ and $\theta = 73.4°$. These values imply that the molecular chain is inclined toward both the a_s- and the b_s-axes, while the inclination is slightly enhanced in the b_s-axis

TABLE 1: Comparison of the Band Frequencies of the β'_1-Form of PPM Measured by the Normal Incident Transmission Method (87 K) and RAS (297 K) with Those of the β-Forms of MMM and PPP[a]

PPM β'_1			MMM β		PPP β	
transmission[b] (cm^{-1})	RAS (cm^{-1})	assignment[d]	transmission[b] (cm^{-1})	assignment[d]	transmission[b] (cm^{-1})	assignment[d]
1152.1(vw)			1163.3(w)		1163.2(vw)	
1162.3(vw)			1174.0(m)	T1-t	1174.0(w)	T1-t
1172.8(VS)			1182.3(m)	W1-t	1181.2(m)	W1-t
1181.4(S)	1179.7	W1-t(M,P)	1185.3(m)	T1-g	1185.5(w)	T1-g
1193.0(m)		W2-t(M)	1198.6(m)	T2-t	1194.6(m)	
1194.6(S)		**W1-g(P)**	**1202.4(m)**	**W1-g**	**1197.2(m)**	**W1-g**
1198.8(S)	1199.9	W2-t(P)	sh	W2-t	1200.3(m)	W2-t
1203.3(vw)		W2-t(M)	1210.5(m)	T2-g	1204.7(m)	T2-g
1216.4(m)		**W2-g(P)**	1224.7(m)	T3-t	1213.2(vw)	T3-t
1219.2(m)	1221.1	W3-t(P)	**1228.4(m)**	**W2-g**	**1216.8(m)**	**W2-g**
1224.6(m)			1231.0(w)	W3-t	1219.5(m)	W3-t
1227.3(w)	1227.4	W3-t(M)	1237.1(m)	T3-g	1227.8(m)	T3-g
1238.6(S)		**W3-g(P)**	1246.2(vw)		1233.6(w)	
1244.1(w)	1244.2	W4-t(P)	1250.5(m)	T4-t	1239.0(m)	T4-t
1246.0(w)			**1254.8(S)**	**W3-g**	**1242.2(m)**	**W3-g**
1253.5(w)			1257.0(m)	W4-t		W4-t
1255.5(w)			1260.6(S)	T4-g	1249.2(m)	T4-g
1257.0(vw)	1255.0	W4-t(M)	1272.6(S)	T5-t	1260.7(m)	T5-t
1261.8(S)		**W4-g(P)**	**1275.8(S)**	**W4-g**	**1263.3(S)**	**W4-g**
1267.6(w)	1266.1	W5-t(P)	1280.0(S)	W5-t,T5-g	1268.8(S)	T5-g,W5-t
1278.2(S)		**W5-g(p)**	1290.1(m)	T6-g	1278.3(m)	T6-g
1280.4(w)	1280.4	W5-t(M)	**1295.7(S)**	**W5-g**	**1282.1(S)**	**W5-g**
1288.5(w)	sh[c]	W6-t(P)	1306.8(vw)	W6-t	1287.3(vw)	W6-t
1295.8(w)			1311.0(vw)		**1300.3(S)**	**W6-g**
1301.7(m)		**W6-g(P)**	**1319.2(S)**	**W6-g**	1306.9(vw)	W7-t
1306.1(w)	1306.1	W6-t(M)	1331.4(vw)	W7-t	1313.6(vw)	
1309.5(w)		W7-t(P)	**1339.3(S)**	**W7-g**	**1321.4(m)**	**W7-g**
1322.0(w)	**1320.9**	**W7-g(P)**	1351.1(vw)	W8-t	1331.9(vw)	W8-t
1332.8(w)	1330.2	W8-t(P), W7-t(M)			**1339.6(m)**	**W8-g**
1338.6vw)	**1340.7**	**W8-g(P)**			1349.5(vw)	W9-t
	1347.4					

[a] The transmission bands listed here correspond to those observed in the polarized spectra (Figure 5C). The assignments of the ν_3 progression bands of the β'_1-form in the region of 1350−1150 cm^{-1} are indicated. [b] VS; very strong; S, strong; m, medium; w, weak; vw, very weak. [c] sh, shoulder. [d] W, ν_3 mode; T, ν_7 mode; t, straight chain; g, bent chain; P, palmitoyl; M, myristoyl.

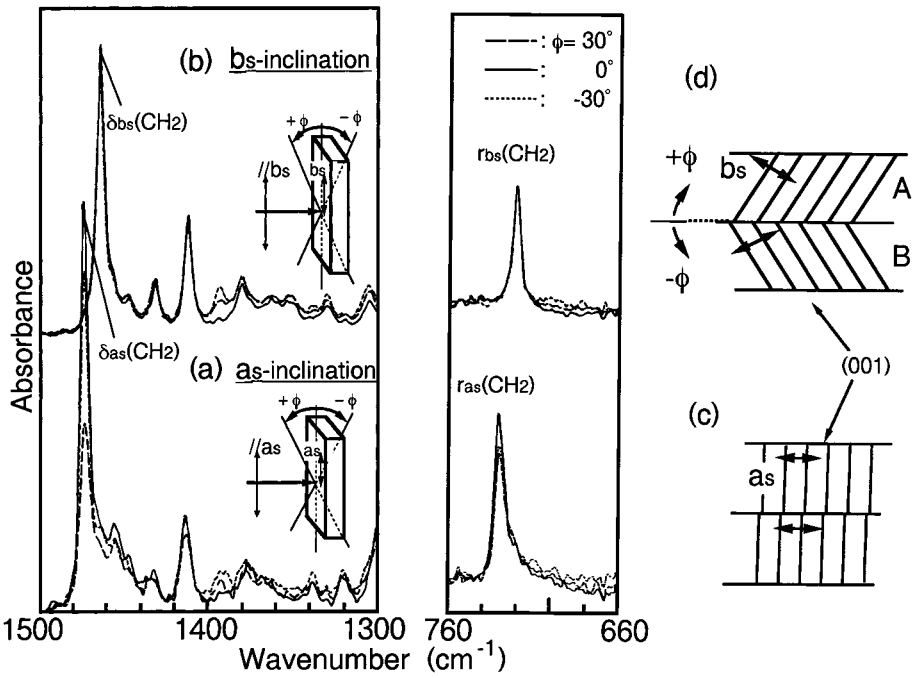

Figure 6. Oblique transmission spectra of the β'_1-form (a and b) and the schematic representations of the inclination directions of the acyl chains (c and d). The tilting directions of the specimen are (a) parallel to the a_s-axis (a_s-inclination) and (b) parallel to the b_s-axis (b_s-inclination).

compared with the a_s-axis. The ϕ value of 18.6°, which is the angle between the *z*-axis and the molecular axis, was calculated from eq 9. Assuming that the molecular chain length is 4.3 nm (in the case of Figure 4c), we roughly estimated the inclination angle of the molecular axis with respect to the (001) plane from the results of the *d*(001) spacing (4.02 nm). The ϕ value of 20.8° obtained from the XRD method satisfactorily agrees with the result obtained from the ATR method.

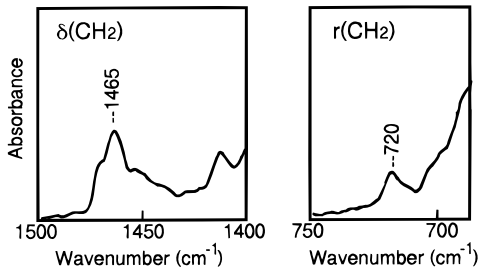

Figure 7. $\delta(CH_2)$ and $r(CH_2)$ bands of the β'_1-form measured by RAS.

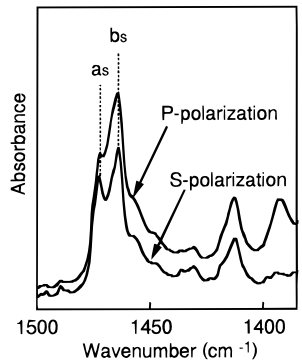

Figure 8. Polarized ATR spectra of the specimen built up on IRE.

TABLE 2: Molecular Orientation in the β'_1-Form Obtained from the ATR Spectra

wavenumber (cm^{-1})	k_x (=k_y)	k_z	k_z/k_x	angle (deg)
1473	0.0433	0.0016	0.0370	$\epsilon = 82.3$
1463	0.0493	0.0088	0.1785	$\theta = 73.4$

Discussion

Molecular Conformation of the β'_1-Form. The preferred acyl chain conformation of the β'_1-form was obtained by analyzing the methylene progression bands of the ν_3 branch modes; the β'_1-form consists of one straight palmitoyl and one straight myristoyl chain and one bent palmitoyl chain. This agrees with acyl chain configurations of type a, b, c, or e in Figure 4. Among these models, we could not determine the absolute configuration of the two straight chains: which chain, myristoyl or palmitoyl, is adjacent to the bent palmitoyl chain and which glycerol configuration, *sn*-1,2 (or *sn*-2,3) or *sn*-1,3 configuration, is most conceivable.

Detailed band assignments of the carbonyl stretch bands (ν(C═O)) may be most determinative to solve this problem, since the frequencies and polarization directions of these bands are directly related to the glycerol configuration. This remains a future work. However, a comparison of the β'_1-bands with those of the PPP β'-form in the region of 1800−1600 cm^{-1} indicated the homology of these crystal structures (Figure 9). Although the ν(C═O) bands are very sensitive to the glycerol conformation, these two forms have common characteristics in the polarization direction and the band frequencies at 1741 cm^{-1} and 1728−1730 cm^{-1}. In the monoacid TAGs, the β'-form transforms to the β-form in solid state, and the glycerol configuration of β takes the *sn*-1,2 configuration having the glycerol structure of type c in Figure 4, as concluded on the basis of the X-ray crystal analysis.[6,7] It is reasonable to assume that no drastic conversion of the glycerol configuration occurs during the β'-to-β-transition. Therefore, the configuration of β-form of monoacid TAGs may also apply to the present case of β'_1. Consequently, type c in Figure 4 is the most probable glycerol configuration for β'_1. In this structure, the methyl end terrace is placed in a relatively flat lamellar interface, giving rise to a stabilized methyl end packing. This may be one reason for the absence of the more stable β-form in PPM.

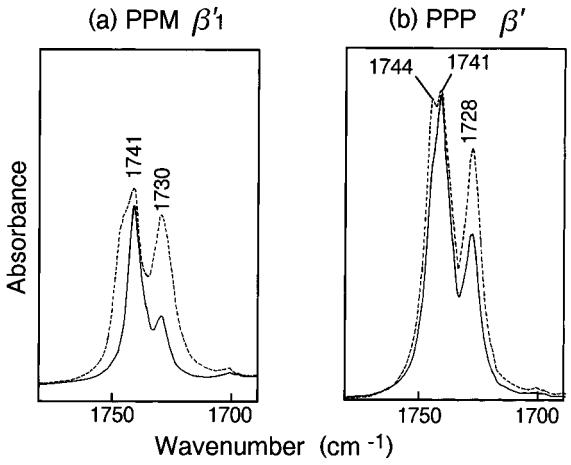

Figure 9. ν(C═O) bands of (a) the β'_1-form of PPM measured by the single crystal and (b) the β'-form of PPP measured by the well-oriented specimen.

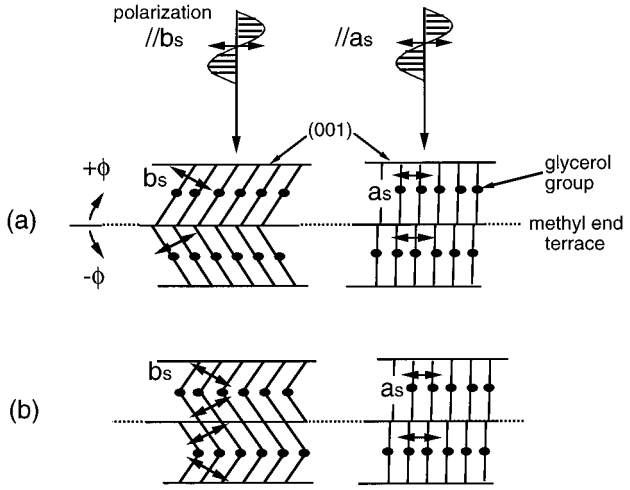

Figure 10. Layer-stacking modes of the β'_1-form. The arrows indicate the direction of the transition dipole moment of the $\delta(CH_2)$ bands.

As for the layer-stacking modes, the previous researchers proposed two possibilities, based on the X-ray diffraction method, which have been a paradox concerning the β'-structure: whether the chain tilt direction alternates at the glycerol group region[24] or at the methyl end terrace.[25] The present results of the oblique transmission experiments indicated that the acyl chains tilt toward both the b_s- and a_s-axes with respect to the (001) plane (Figure 10). The degree of inclination toward the b_s-axis is larger than that of the a_s-axis. Concerning the problem of the layer-stacking modes, we confirmed that the acyl chains are stacked in a unidirectional manner toward the a_s-axis, while they are inclined alternately along the successive layer toward the b_s-axis. However, we could not clarify the two possibilities of the stacking modes described above. The differentiation of type a or b in Figure 10 needs further work by X-ray single-crystal analysis.

Additional information obtained from the polarization properties of the transmission spectra (Figure 5A(a)) is that the spectra measured by intermediate polarization direction (45° and 135°) between a_s‖ (0°) and b_s‖ (90°) did not have the same feature. It means that there is no specific symmetry in the (001) plane. Therefore, the crystal structure of β'_1 assumes a triclinic unit cell with the $O_\perp$ subcell as observed in the B′-form of odd-numbered fatty acids.[26,27]

Subcell Arrangement. On the basis of the previous X-ray diffraction studies,[6,7] TAG molecules take a chair conformation with one hydrocarbon chain pointing in one direction opposite to the others. This is the common feature throughout all crystal forms of TAGs. Two chairs form a dimeric unit that seems to remain unchanged through the polymorphic transition from β' to β in monoacid TAGs. In the β'-type form, packing in the $O_\perp$ subcell while keeping the dimeric units is geometrically limited to arrange in one lamella. One dimeric unit includes three acyl chains in the lateral direction as illustrated in Figure 4. Since the repeating period of lateral direction with the $O_\perp$ subcell cannot consist of three chains, the unit cell should involve at least two dimeric units. Therefore, the problems to be solved are the shape of dimeric units and their arrangement manner. The clarification of it needs further work using X-ray single-crystal analysis.

Utility of the ν_3 Progression Bands as a Structural Indicator. In Part I,[1] we assigned the ν_3, ν_7, and ν_8 progression bands of monoacid TAG β-forms. The ν_7 and ν_8 bands include the dipole moments perpendicular to the chain axis, which is ascribed to the CH_2 rocking modes. On the other hand, the transition dipole moments of the ν_3 bands are parallel to the chain axis due to the CH_2 wagging modes. Among these three progression bands, we considered that the ν_3 bands are suitable to examine the acyl chain conformation. The reasons are (1) the intensity of both ν_3 bands arising from the straight and the bent chains is strong, and (2) these bands are not very sensitive to the subcell structure.

The first point was described in Part I.[1] As for the second reason, the interactions in the lateral directions are very weak compared with modes of perpendicular displacements, since the displacements of the ν_3 progression bands are parallel to the chain axis. For example, Figure 11 shows the comparison of the IR spectrum of PPP β having a $T_\parallel$ subcell with that of β' having a $O_\perp$ subcell. The marked bands with open circles and closed circles in the β-form are because of the ν_3 progression bands of the *sn*-3 and *sn*-1,2 chains, respectively. A comparison of the progression bands of β' with β indicated that there were no significant differences in frequencies of the ν_3 bands between the two forms. Therefore, one can use the ν_3 progression bands as the reference bands to clarify the acyl chain configuration of the mixed-acid TAGs.

On the contrary, the polarization direction and the intensity of the progression bands were strongly influenced by the polymorphic form. Concerning the polarization dependence, the ν_3 bands arising from the bent chain of the β-form clearly appeared in both of the transmission spectra (Figure 11c) and RAS (Figure 11d), while those of β'-type were observed mainly in the transmission spectra (Figure 5A(a)). As for the band intensity, the ν_7 bands due to the *sn*-3 chains marked with arrows in Figure 11c could not be measured clearly in the β'-form of PPP (Figure 11a). In the same way, those bands were very weak in the case of the PPM β'_1-form. This discrepancy of the band intensity between β' and β may be not only due to the inclination degree of the molecular axis against the (001) plane but also due to the structural difference in the relative position between the esterified bond and hydrocarbon plane of the *sn*-3 chain. The consideration may be rationalized by the fact that the progression bands were strongly dependent on the C−O stretch (ν(C−O)) modes of the carboxyl group esterified to the glycerol backbone.[28] On the other hand, the intensity of the ν_3 bands were less sensitive to the polymorphic form.

Concluding Remarks

The detailed assignments of IR bands carried out in Part I were found to be quite useful in assessing the molecular structures of TAGs, which are barely examined by the X-ray structure analysis using high-quality single crystals. The main features of the molecular structure of the PPM β'_1-form obtained by several IR techniques are summarized in the following:

(1) The three acyl chains consist of the straight palmitoyl and myristoyl chains and the bent palmitoyl chain.

(2) The acyl chains are packed in $O_\perp$ subcell, and the projection of the a_s- and b_s-axes are perpendicular and parallel to the long axis of the parallelogram-shaped crystal, respectively.

(3) The molecules are inclined with respect to the (001) plane; the degree of inclination toward the b_s-axis is larger than that toward the a_s-axis. The molecular stacking sequence along the successive layer is unidirectional toward the a_s-axis, while alternately toward the b_s-axis.

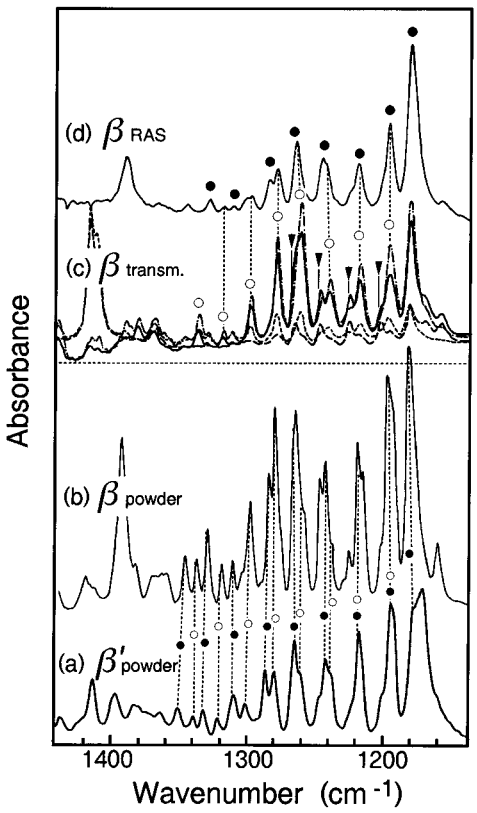

Figure 11. IR spectra of tripalmitin: nonpolarized transmission spectra of (a) β and (b) β', polarized transmission spectra of (c) β, and RAS of (d) β. In (a) and (b), the bands connected with the dotted lines are the ν_3 progression bands of the *sn*-1,2 straight chains and the *sn*-3 bent chains. In (c) and (d), the marked bands with arrows, open circles, and closed circles indicate the ν_7 bands of the bent chain, the ν_3 bands of the *sn*-1,2 chains, and those of the *sn*-3 chain, respectively.

Acknowledgment. We thank Ichiro Tobita of Rigaku Co. for his experimental support.

References and Notes

(1) Yano, J.; Kaneko, F.; Kobayashi, M.; Sato, K. *J. Phys. Chem. B* **1997**, *101*, 8110.

(2) Calaghan, P. T.; Jolly, K. W. *Chem. Phys. Lipids* **1977**, *19*, 56.

(3) Fahey, D. A.; Small, D. M. *Biochemistry* **1986**, *25*, 4468.

(4) Hagemann, J. W. *Crystallization and Polymorphism of Fats and Fatty Acids*; Garti, N., Sato, K. Eds.; Marcel Dekker: New York, 1988; pp 9−95.

(5) Small, D. M. *The Physical Chemistry of Lipids*; Plenum: New York, 1986; pp 345−394.

(6) Larsson, K. *Ark. Kemi* **1964**, *23*, 1.

(7) Jensen, L. H.; Mabis, A. J. *Nature (London)* **1963**, *197*, 681.

(8) Sato, K. *Applied Lipid Research*; Padley, F., Ed.; JAI Press Inc.: Greenwich, CT, 1996; Vol. 2, pp 213−268.

(9) Bociek, S. M.; Ablett, S.; Norton, I. T. *J. Am. Oil Chem. Soc.* **1985**, *62*, 1261.

(10) Eads, T. M.; Blaurock, A. E.; Bryant, R. G.; Roy, D. J.; Croasman, W. R. *J. Am. Oil Chem. Soc.* **1992**, *69*, 1057.

(11) Kodali, D. R.; Atkinson, D.; Small, D. M. *J. Phys. Chem.* **1989**, *93*, 4683.

(12) Kodali, D. R.; Atkinson, D.; Small, D. M. *J. Lipid Res.* **1990**, *31*, 1853.

(13) Kodali, D. R.; Atkinson, D.; Redgrave, T. G.; Small, D. M. *J. Am. Oil Chem. Soc.* **1984**, *61*, 1078.

(14) Kodali, D. R.; Atkinson, D.; Small, D. M. *J. Dispersion Sci. Technol.* **1984**, *10*, 393.

(15) Kaneko, F.; Shirai, O.; Miyamoto, H.; Kobayashi, M.; Suzuki, M. *J. Phys. Chem.* **1994**, *98*, 2185.

(16) Kaneko, F.; Ishikawa, E.; Kobayashi, M.; Suzuki, M. *Rep. Prog. Polym. Phys. Jpn.* **1994**, *37*, 241.

(17) Fraser, R. D. B. *J. Phys. Chem.* **1953**, *21*, 1511. Fraser, R. D. B. *J. Chem. Phys.* **1958**, *29*, 1428. Fraser, R. D. B. *J. Chem. Phys.* **1958**, *28*, 1113.

(18) Higashiyama, T.; Takenaka, T. *J. Phys. Chem.* **1974**, *78*, 941.

(19) Flournoy, P. A.; Schaffers, W. J. *Spectrochim. Acta* **1966**, *22*, 5.

(20) Flournoy, P. A. *Spectrochim. Acta* **1966**, *22*, 15.

(21) The value of n_2, 1.5, was obtained from interference fringes using the following equation; $nD = m/[2(\bar{\nu}_1 - \bar{\nu}_2)]$ where n is the refractive index, D is the cell length, $\bar{\nu}_1$ and $\bar{\nu}_2$ are two wavenumbers, and m is the number of interference fringes between $\bar{\nu}_1$ and $\bar{\nu}_2$.

(22) Kobayashi, M. In ref 4, pp 139−187.

(23) Bunn, C. W. *Trans. Faraday Soc.* **1939**, *35*, 482.

(24) Precht, von D.; Frede, E. *Kiel. Milchwirtscha. Forschungsber.* **1977**, *29*, 265.

(25) Hernqvist, J. L. In ref 4, pp 97−137.

(26) Goto, M.; Asada, E. *Bull. Chem. Soc. Jpn.* **1984**, *57*, 1145.

(27) von Sydow, E. *Acta Crystallogr.* **1954**, *7*, 823.

(28) Tasumi, M.; Shimanouchi, T.; Watanabe, A.; Goto, R. *Spectrochim. Acta* **1964**, *20*, 629.